Cobalt-based age models of pelagic clay in the South Pacific Gyre

Citation	Dunlea, A. G., Murray, R. W., Sauvage, J., Pockalny, R. A., Spivack, A. J., Harris, R. N., & D'Hondt, S. (2015). Cobalt-based age models of pelagic clay in the South Pacific Gyre. Geochemistry, Geophysics, Geosystems, 16(8), 2694-2710. doi:10.1002/2015GC005892
DOI	10.1002/2015GC005892
Publisher	John Wiley & Sons, Inc.
Version	Version of Record
Terms of Use	http://cdss.library.oregonstate.edu/sa-termsofuse

AGU PUBLICATIONS

Geochemistry, Geophysics, Geosystems

RESEARCH ARTICLE
10.1002/2015GC005892

Cobalt-based age models of pelagic clay in the South Pacific Gyre

Ann G. Dunlea[1], Richard W. Murray[1], Justine Sauvage[2], Robert A. Pockalny[2], Arthur J. Spivack[2], Robert N. Harris[3], and Steven D'Hondt[2]

[1]Department of Earth and Environment, Boston University, Boston, Massachusetts, USA, [2]Graduate School of Oceanography, University of Rhode Island, Narragansett, Rhode Island, USA, [3]College of Earth, Ocean, and Atmospheric Sciences, Oregon State University, Corvallis, Oregon, USA

Key Points:
- Improved methodology to dating pelagic clay
- Spatial variability of Co in seawater reflected in sediment
- Age models for pelagic clay from the South Pacific Gyre

Supporting Information:
- Supporting Information S1
- Figure S1
- Table S1

Correspondence to:
A. G. Dunlea,
adunlea@bu.edu

Citation:
Dunlea, A. G., R. W. Murray, J. Sauvage, R. A. Pockalny, A. J. Spivack, R. N. Harris, and S. D'Hondt (2015), Cobalt-based age models of pelagic clay in the South Pacific Gyre, *Geochem. Geophys. Geosyst.*, *16*, 2694–2710, doi:10.1002/2015GC005892.

Received 5 MAY 2015
Accepted 24 JUL 2015
Accepted article online 29 JUL 2015
Published online 21 AUG 2015

Abstract Dating pelagic clay can be a challenge due to its slow sedimentation rate, post-depositional alteration, and lack of biogenic deposition. Co-based dating techniques have the potential to create age models in pelagic clay under the assumption that the flux of non-detrital Co to the seafloor is spatially and temporally constant, resulting in the non-detrital Co concentrations being inversely proportional to sedimentation rate. We apply a Co-based method to the pelagic clay sequences from Sites U1365, U1366, U1369, and U1370 drilled during Integrated Ocean Drilling Program (IODP) Expedition 329 in the South Pacific Gyre. We distinguished non-detrital Co from detrital Co using multivariate statistical partitioning techniques. We found that the non-detrital flux of Co at Site U1370 is approximately twice as high as that at the other sites, implying that the non-detrital Co flux is not regionally constant. This regional variation reflects the heterogeneous distribution of Co in the water column, as is observed in the present day. We present an improved approach to Co-based age modeling throughout the South Pacific Gyre and determine that the Co-based method can effectively date oxygenated pelagic clay deposited in the distal open ocean, but is less reliable for deposition closer to continents. When extending the method to geologically old sediment, it is important to consider the paleolocation of a given site to ensure these conditions are met.

1. Introduction

Dating pelagic clay is a challenge for paleoceanographic studies, due to its low accumulation rate, postdepositional alteration, and lack of appropriate material for detailed biochronology. However, the composition of pelagic clay exhibits subtle variations associated with provenance that can be related to changes in tectonic, chemical, and biological factors influencing open ocean sedimentary environments. To put these changes in a paleoceanographic context and correlate open ocean variations with global climate events requires robust age modeling. Although pelagic clay sequences have proven to be an important archive of ocean history over long time scales (0–85 Myr) [e.g., *Rea and Bloomstine*, 1986; *Leinen*, 1989; *Zhou and Kyte*, 1992; *Kyte et al*., 1993; *Gleason et al*., 2002; *Stancin et al*., 2008a, 2008b], such models have been difficult to construct. A standardized technique to date pelagic clay would greatly increase its use in paleoceanography and paleoclimatology.

Techniques based on ^{230}Th and ^{10}Be have been used to date pelagic clay, but are limited to relatively short time spans (~0.5 and 8 Myr, respectively), that can translate to a few tens of centimeters in regions with extremely low sedimentation rates [e.g., *Kadko*, 1985; *Bourles et al*., 1989; *Marcantonio et al*., 1996; *Frank et al*., 2008]. For deeper time, ichthyology [e.g., *Ingram*, 1995; *Martin and Haley*, 2000; *Gleason et al*., 2002], magnetostratigraphy [e.g., *Backman et al*., 2008], and authigenic Os isotopic techniques [e.g., *Peucker-Ehrenbrink et al*., 1995; *Klemm et al*., 2005; *Ravizza*, 2007] have been employed to provide discrete age dates. Each of these approaches has strengths and weaknesses. Most importantly, however, they only provide discrete age points between which linear sedimentation rates are often assumed. Due to slow sedimentation rates, such tie points are often spaced far apart in age.

A Co-based dating technique, can be the foundation for age modeling of pelagic clay and Fe-Mn crust and nodules, by determining instantaneous sedimentation rates on a sample-by-sample basis. This is a great advantage compared to other techniques that rely on linear interpolations between stratigraphically spaced

Table 1. Summary of IODP Sites Examined in This Study [*D'Hondt et al.*, 2011]

Site	Latitude	Longitude	Water Depth (m)	Total Sediment Thickness (m)	Polarity Chron Age Range (Ma)	Tectonic Reconstruction Estimate (Ma)
U1365	−23°51′	−165°39′	5697	75.6	84–124.6	100
U1366	−26°03′	−156°54′	5127	34	84–124.6	95
U1367	−26°29′	−137°56′	4285	22	33.3–33.7	33.5
U1369	−39°19′	−139°48′	5283	16	57.2–58.4	58
U1370	−41°51′	−153°06′	5076	73	73.6–79.5	75
U1371	−45°58′	−163°11′	5306	132	71.5–72.9	73

control points. While Co-based age models are widely cited, their use in marine sediment is, in fact, relatively infrequent [*Krishnaswami*, 1976; *Kadko*, 1985; *Zhou and Kyte*, 1992; *Kyte et al.*, 1993; *Dalai and Ravizza*, 2006]. Their application to ferromanganese crusts and nodules is relatively more common [*Halbach et al.*, 1982, 1983; *Manheim and Lane-Bostwick*, 1988; *Puteanus and Halbach*, 1988; *McMurtry et al.*, 1994; *Banakar et al.*, 1997; *Frank et al.*, 1999; *van de Flierdt et al.*, 2004; *Klemm et al.*, 2005; *Li et al.*, 2008; *Hein et al.*, 2012].

Co-based techniques assume that the flux of non-detrital Co to the seafloor is spatially and temporally constant. Thus, high concentrations of non-detrital Co indicate slow sedimentation rates and vice versa. Other techniques to determine instantaneous sedimentation rates of pelagic sediment in deep time include Ir and ^{3}He. Ir is thought to behave similarly to Co, except at the K-Pg boundary [e.g., *Zhou and Kyte*, 1992; *Kyte et al.*, 1993; *Dalai and Ravizza*, 2006]. Extraterrestrial ^{3}He in pelagic sediment is sometimes proven to be constant enough to determine sedimentation rates [e.g., *Marcantonio et al.*, 1996; *Paquay et al.*, 2014], but in other studies has shown to be variable [e.g., *Farley*, 1995; *Farley et al.*, 2012]. Many of the studies examining the variable flux of ^{3}He (and also extraterrestrial Os isotopes) in deep-sea pelagic clay [e.g., *Farley*, 1995; *Pegram and Turekian*, 1999] developed using samples from Core LL44-GPC3 and use a Co-based age model [*Kyte et al.*, 1993] to ground truth their conclusions. These studies assume the flux of non-detrital Co to be "constant," and "hydrogenous" or "authigenic" in origin, being sourced directly from seawater.

We assess the accuracy of these assumptions in Co-based dating techniques and discuss why the flux of non-detrital Co to the seafloor may seem to be approximately "constant," particularly at a single location, even when Co concentrations are not well mixed in the ocean [e.g., *Saito and Moffett*, 2002]. We improve the understanding and quantify the uncertainties associated with use of Co-based age models. These uncertainties can be large. They are best identified by working with material from multiple locations to separate local from regional influences on Co accumulation and to determine the effectiveness and limitations of Co-based methods overall. We produce a relatively high-resolution age model to 65.5, 95, 58, and 65.5 Ma for the pelagic clay sequences of Sites U1365, U1366, U1369, and U1370, respectively, drilled during Integrated Ocean Drilling Program (IODP) Expedition 329 in the South Pacific Gyre (SPG). In addition to developing age models for these particular IODP sites, we provide an analytical and numerical roadmap for other researchers to apply Co-based accumulation rate models to different pelagic locations around the global ocean.

2. Sampling and Analytical Methods

Six of the seven sites (Table 1) drilled to basement during IODP Expedition 329 (U1365–U1370) are mostly composed of oxic [*Fischer et al.*, 2009; *D'Hondt et al.*, 2011, 2015], homogenous, brown pelagic clay (Figure 1). Average sedimentation rates calculated from total sediment thickness and approximate basement age at each site are extremely low, ranging from 0.3 to 1 m/Myr [*D'Hondt et al.*, 2009, 2011, 2015]. The seventh site (Site U1371) is mostly siliceous ooze [*D'Hondt et al.*, 2011]. This study focuses primarily on Sites U1365, U1366, U1369, and U1370, which are exclusively pelagic clay except for a thick chert interval from 44 to 62 meters below seafloor (mbsf) at Site U1365, and a thin carbonate interval from 62 to 63 mbsf at Site U1370. The pelagic clay portions of Sites U1367 (shallower than the carbonate interval) and U1371 (deeper than the siliceous interval) are also included in part of this study but the sampling resolution is too low for age model determinations.

Details of the analytical geochemical procedures are presented in *Dunlea et al.* [2015]. In brief, samples consist of sediment squeeze cakes remaining after porewater extractions performed on the IODP drillship R/V *JOIDES Resolution* [*D'Hondt et al.*, 2011]. Sample preparation, digestions, and analysis were conducted at

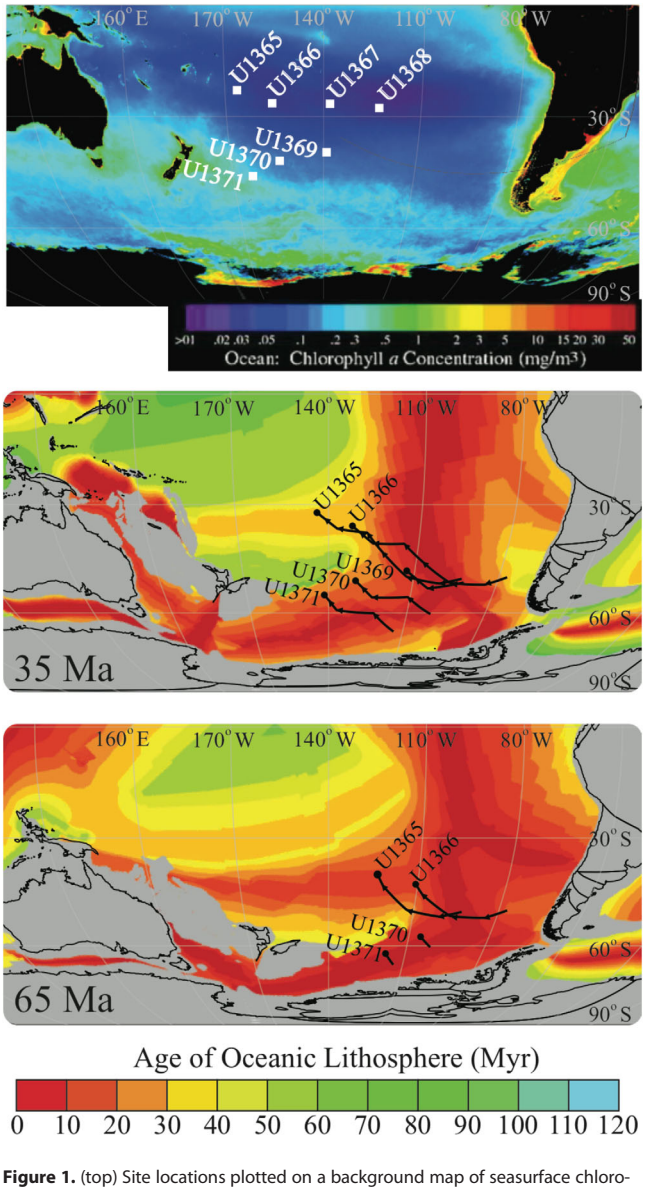

Figure 1. (top) Site locations plotted on a background map of seasurface chlorophyll concentrations (http://oceancolor.gsfc.nasa.gov/SeaWiFS/). (middle and bottom) Sites with backtrack paths [*Seton et al*., 2012; *Gurnis et al*., 2012] against age of oceanic lithosphere [*Müller et al*., 2008] at 35 and 65 Ma. Paths are plotted against a latitude/longitude reference frame, and thus appear to cross the East Pacific Rise, when in reality each site's history has entirely been on the Pacific Plate.

Boston University. Sediment samples were freeze-dried and hand-powdered with an agate mortar and pestle. For major and certain trace elements, sample powders were digested by flux fusion [*Murray et al*., 2000] and analyzed by inductively coupled plasma-emission spectrometry (ICP-ES). For analysis of further trace and rare earth elements, including Co, sample powders were dissolved in a heated acid cocktail (HNO_3, HCl, and HF, with later additions of HNO_3 and H_2O_2 after samples were dried down) under clean-lab conditions and analyzed by inductively couple plasma-mass spectrometry (ICP-MS). The protocol was similar to that described in *Scudder et al*. [2014] and is detailed in *Dunlea et al*. [2015]. Three separate digestions of an in-house SPG sediment standard were analyzed with each batch and determined precision [(average)/(standard deviation) × 100] was ∼2% or better of the measured value for each element. The international Standard Reference Material BHVO-2 was analyzed as an unknown with each batch and results were consistently found to be accurate within precision for each element [*Ireland et al*., 2014].

3. Defining the Language: "Constant" Co, Non-detrital Co, Authigenic, Hydrogenous

As cited above, several previous studies have employed Co-based accumulation rates for marine sediment, Fe-Mn nodules, and Fe-Mn crust. Particularly in marine sediment, terminology such as "Constant-Co" (or a slight variation thereof) is commonly used. Implicit in the use of this term is the assumption that the flux of Co to the seafloor is constant, either globally or at least over very large distances (e.g., ocean-basin scale). Thus, the term "Constant-Co" includes an interpretation from the outset. Because we will show that such constancy is not the case, we instead use the term "Co-based," which does not imply any process or distribution pattern. We prefer this term because it is more objective, and only refers to the chemical element used in the age models.

We further show that the crux of constructing Co-based age models is, on a per sample basis, determining what fraction of the total Co is contributed by non-biogenic *detrital* inputs (e.g., eolian dust, other terrigenous inputs, volcanic ash, altered eroded basalt, etc.) and what fraction of the total Co is contributed by the sum of the other sources (e.g., authigenic uptake, hydrogenous precipitation, etc.) which are, by closure, *non-detrital*. For the purposes of Co-based accumulation rates, therefore, the most important partitioning is between detrital Co (which cannot be part of a Co-based accumulation model) and the total non-detrital Co

(upon which a Co-based age model is wholly based), regardless of which phase currently hosts this non-detrital Co. Therefore, and aware of extensive discussions in the literature about the variety of processes by which authigenic and hydrogenous phases may form, we simply refer to the Co that is relevant to Co-based accumulation rate models as non-detrital Co.

4. Pathways of Co to Deep Pelagic Sediment

Previous studies using a constant Co flux method (hereinafter referred to as "Co-based," as above) refer to the Co deposited on the seafloor at a constant rate as being "authigenic" or "hydrogenous" (hereinafter, part of "non-detrital Co," as above). This historical terminology implies specific pathways by which Co becomes part of the bulk sediment. However, such labels neglect the primary origin and distribution of the Co, which is of utmost importance when developing a Co-based age model. Here we explore two questions that address this, namely: why and how is Co deposited in marine sediment? and, how constant is "constant"?

4.1. Sources of Co to the Water Column

Ongoing water-column research is rapidly improving our understanding of the supply to and distribution of Co in the ocean. We briefly review the sources of Co to the ocean, focusing on how they may affect the distribution of Co in the water column overlying pelagic clay in the open ocean.

Eolian dust and volcanic ash are removed to the seafloor quite rapidly and do not supply a spatially constant nor large flux of Co across all ocean basins over time. Eolian dust and volcanic ash influence Co concentrations in the surface waters close to continents [*Dulaquais et al*., 2014a, 2014b], but they are likely to be an insignificant source in the open ocean [*Shelley et al*., 2012]. For example, in the South Atlantic, eolian material is estimated to contribute $<$1% of the Co in the water column [*Noble et al*., 2012]. The solubility of Co in natural dust is low (0.14%) [*Thurocszy et al*., 2010], but even if it were more soluble, even by an order of magnitude, the contributions of eolian Co would still be relatively quite small compared to other sources in the open ocean [*Noble et al*., 2012].

Hydrothermal fluids are enriched in Co relative to seawater (20–230 nM versus 0.03 nM) [*Von Damm et al*., 1985], but hydrothermal Co precipitates very close to the ridge axis [*German et al*., 1990; *Noble et al*, 2008, 2012] and even if it traveled far would only comprise $\sim$2.4% of the total Co flux to the global oceans [*Swanner et al*., 2014]. In the pre-Cambrian, anoxic oceans may have caused Co from hydrothermal vents to disperse further through the water column [*Swanner et al*., 2014], but in present-day oxygenated oceans it is removed very rapidly close to the ridge.

Micrometeorites could contribute a continuous flux of Co to the seafloor, but even the highest estimate of 270 metric tons of cosmic dust accreted to Earth every day [*Plane*, 2012] explains only $\sim$0.5% of the non-detrital Co flux to the seafloor, assuming typical micrometeorites have an average chondritic composition (500 μg/g Co) [*McDonough and Sun*, 1995]. Interestingly, Co correlates well with Ir, a common cosmogenic tracer [*Dalai and Ravizza*, 2006], at multiple sites except at the K-Pg Boundary where Ir concentrations spike upward and Co concentrations show little change [*Kyte and Wasson*, 1986; *Zhou and Kyte*, 1992; *Kyte et al*., 1993]. While the correlation between Ir and Co in non-K-Pg sediment is consistent with a cosmogenic origin of Co, it is interpreted as more likely resulting from similar behavior of Ir and Co during authigenesis [*Dalai and Ravizza*, 2006].

Rivers supply large amounts of Co to the continental margins [*Swanner et al*., 2014], but the Co is very particle reactive and deposited on the continental shelf. When this sediment becomes anoxic, dissolved Mn, Fe, and Co are released into the water column as metal-bearing mineral phases are reduced [*Noble et al*., 2012].

Anoxic sediment along the continental margin is the main source of dissolved Co to the open ocean [*Noble et al*., 2012]. In the South Atlantic Ocean, the dissolved Co plume is transported thousands of kilometers toward the centers of gyres with the highest Co concentrations traveling at the depth of the oxygen minimum zone (OMZ, $<$100 μmol O_2/kg) and decreasing further from the continent [*Noble et al*., 2012]. The total Co concentration is found to be inversely proportional to oxygen concentrations between 300 and 800 meters in the South Atlantic water column [*Noble et al*., 2012] and ongoing studies of Co concentration transects across the South Pacific will reveal if Co behaves similarly in the SPG.

4.2. Co Behavior in the Water Column

Co is not well mixed in the ocean, with whole-ocean residence times on the order of 40–150 years [*Saito and Moffett*, 2002; *Aparicio-González et al*., 2012]. The concentration of Co in seawater ranges from ~4 to 120 pM, occurring primarily as Co^{2+} ions and its chloro-, sulfato-, and carbonato- complexes [*Nolan et al*., 1992]. Co is a micronutrient, a structural component of vitamin B_{12}, and may be co-limiting in some regions [*Saito and Moffett*, 2001; *Noble et al*., 2012; *Shelley et al*., 2012].

As succinctly described by *Noble et al*. [2012, p. 989], the water column profiles of "iron, cobalt, and manganese fall into the hybrid-type category since their distributions are controlled by a combination of phytoplankton uptake, which creates nutrient-like distributions in the photic zone, and scavenging, which creates scavenged-like distributions in intermediate and deep waters." Ongoing studies of the complexities of Co removal are examining several different mechanisms, including co-precipitation with Mn-oxides and biological export to the seafloor [*Swanner et al*., 2014, and references therein].

Deeper than the OMZ in the open ocean, Co concentrations show smaller gradients and are relatively homogenous across the ocean basin [*Noble et al*., 2012; *Dulaquais et al*., 2014b]. Organic complexing of Co reduces the scavenging rate [*Saito and Moffett*, 2001] and possibly explains how Co can become dispersed throughout and relatively well mixed in the deeper ocean away from continents.

While the exact mechanism that removes Co from seawater to pelagic clay, nodules, and ferromanganese crust is poorly understood, the primary pathway in the open ocean is the settling of Mn-phases that form microbially mediated in the water column and adsorb Co onto their surfaces and/or incorporate Co into their structure [*Knauer et al*., 1982; *Cowen and Bruland*, 1985; *Moffett and Ho*, 1996; *Saito and Moffett*, 2001; *Bown et al*., 2011; *Castrillejo et al*., 2013]. The settling of these Co-bearing Mn-phases to the seafloor is described as a slow, leaky process as they are gradually removed from seawater over time [*Cowen and Bruland*, 1985]. If the removal process is steady and constant, Co concentrations in marine sediment will be inversely proportional to sedimentation rate and may be suitable as a sedimentation rate chronometer.

Very importantly, however, the concentration of Co in the water column is neither evenly distributed across an ocean basin nor does it have a constant concentration of Co through time or space. Export of Co to the seafloor may be higher near continents than in the open ocean, due to higher concentrations of dissolved Co in the OMZ and higher productivity in upwelling regions near the coasts. While it is possible that slow precipitation of Co in the open ocean may be constant enough to act as a chronometer, the water-column Co heterogeneities call into question the assumption that Co-based accumulation rate models can be based on a globally or even regionally precisely constant flux of Co to the seafloor. More research targeting Co removal mechanisms to marine sediment is critical to improve our understanding of the relative importance of the spatial and temporal variability of these processes. Regardless, however, these lines of research clearly indicate that these processes are not constant across ocean basins, which has implications for the use of Co in sediment dating.

5. Co-Based Chronology Calculations

In this study, we create Co-based age models for marine sediment using calculations similar to *Krishnaswami* [1976] and *Kadko* [1985]. Co-based techniques and equations for calculating the growth rate of ferromanganese crusts and nodules cannot be applied to sediment because sediment has Co concentrations that are an order of magnitude lower and contain a detrital component that contributes significant Co abundances.

In marine sediment, the total concentration of Co (Co_t) in the sediment is the sum of the contributions from detrital phases (Co_d) and the sum of the non-detrital phases ($Co_{non\text{-}det.}$). In SPG pelagic clay, Co_t concentrations may be as high as ~500 μg/g (Figure 2a and Table S1), and the Co/Al ratio (ranging 2–100 μg/g, Figure 2b) significantly surpasses that of post-Archean average Australian Shale (PAAS) (23 μg/g Co and 2.3 μg/g Co/Al) [*Taylor and McLennan*, 1985] and mid-ocean ridge basalt (43 μg/g Co and 5.53 μg/g Co/Al) [*Gale et al*., 2013]. Thus, the Co/Al ratios and Co concentration comparisons indicate that the vast majority of the Co in SPG pelagic clay is non-detrital and sourced from elsewhere. We use Al in these ratios because there is no recognizable scavenged Al component [*Murray et al*., 1993; *Murray and Leinen*, 1996] in the SPG pelagic clay [*Dunlea et al*., 2015], due the very high aluminosilicate inventory.

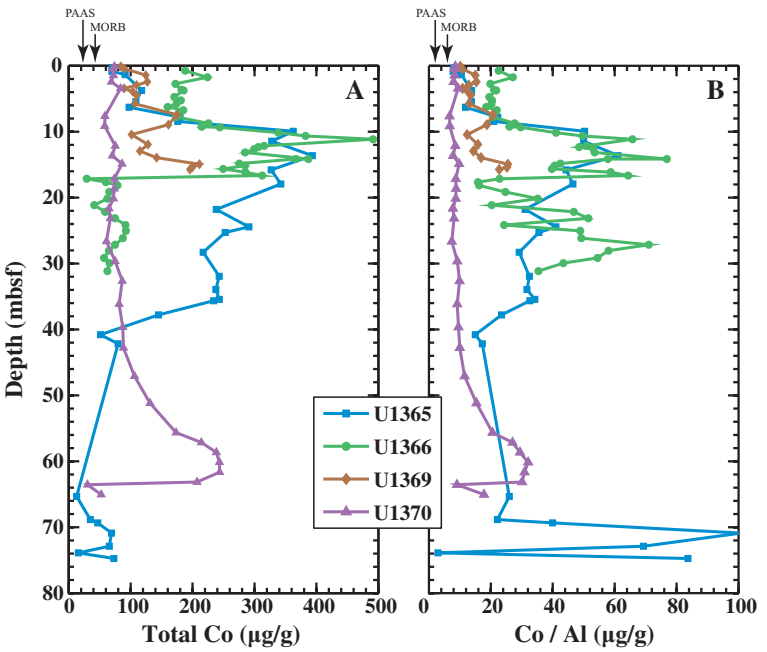

Figure 2. (a) Total Co concentrations in (μg/g) (Co_t, in equation (1)) and (b) Co/Al (μg/g) ratio versus depth (meters below seafloor). Arrow indicates Co concentration (μg/g) and Co/Al (μg/g) of PAAS (23 and 2.3 μg/g) [*Taylor and McLennan*, 1985] and MORB (43 and 5.54 μg/g) [*Gale et al.*, 2013].

Previous studies have used operationally defined chemical leaches to separate detrital Co from putative authigenic Co [e.g., *Krishnaswami*, 1976]. Given the highly altered nature of pelagic clay, however, and the difficulty these leaching techniques have in distinguishing different aluminosilicate materials from each other [e.g., *Ziegler et al.*, 2007], we avoid such leaching. Instead, we determine the amount of detrital Co in each sample by multivariate statistical partitioning [*Miesch*, 1976; *Heath and Dymond*, 1977; *Leinen and Pisias*, 1984; *Zhou and Kyte*, 1992; *Kyte et al.*, 1993; *Ziegler and Murray*, 2007; *Ziegler et al.*, 2008; *Scudder et al.*, 2009, 2014; *Pisias et al.*, 2013]. The partitioning calculations used in this study are detailed in *Dunlea et al.* [2015], and determine the mass fraction of sediment contributed by eolian dust, volcanic ash, apatite, Fe-Mn oxyhydroxides, biogenic silica, and altered basalt, on a sample-by-sample basis. From the compositional mass fractions, we quantify the amount of Co_d collectively sourced from eolian dust and volcanic ash and compare that to the Co_t analyzed in each sample. The difference is $Co_{non\text{-}det.}$, which is the Co upon which the age models are based or, simply:

$$Co_{non\text{-}det.} = Co_t - Co_d \tag{1}$$

Assuming, for now, that the flux of non-detrital Co to the seafloor is constant, $Co_{non\text{-}det.}$ will be inversely related to sedimentation rate,

$$S_i = \frac{K}{Co_{non\text{-}det.,i} \times \rho_i} \tag{2}$$

where for sample *i*,

$Co_{non\text{-}det.,i}$ = concentration of non-detrital Co (μg/g);
S_i = instantaneous sedimentation rate (cm/Myr);
K = non-detrital input rate (μg/cm^2/Myr);
ρ_i = Dry Bulk Density (DBD, g/cm^3).

The latter three of these terms are discussed in sections 5.1 and 5.2.

5.1. Dry Bulk Density (DBD)

For the DBD of each sample (Table S1), we used IODP Expedition 329 shipboard moisture and density (MAD) and gamma ray attenuated (GRA) density data [*D'Hondt et al.*, 2011]. We removed GRA data outliers

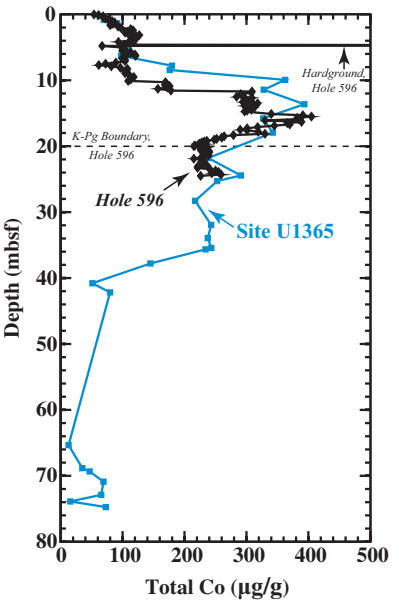

Figure 3. Co concentration (μg/g) versus depth (meters below seafloor) at Site U1365 (from Figure 2) and Hole 596 [*Zhou and Kyte*, 1992]. The position of the K-Pg Boundary in Hole 596 is indicated by black dashed line. Note the slight offset between profiles; when Site U1365 is shifted downward by 2 m, the two profiles match extremely well.

(defined as $\pm$1 standard deviation of the surrounding 50 measurements, covering $\sim$100 cm of core thickness) and took a 50-point moving window average to reduce noise in the GRA trend. GRA density was co-located with the MAD data points and a linear trend was fit to relate the wet GRA density with the dry bulk MAD density at each site individually. This correlation at each site is strong (r^2 between 0.87 and 0.97). Based on the overall GRA-to-DBD relationship, we converted the 50-point moving-point averaged GRA density at the depth of each of the samples to DBD. If MAD data were not from the same hole as the samples, we regressed a line through GRA and MAD data from the same hole and then applied the equation to GRA data co-located with the samples.

5.2. Instantaneous Sedimentation Rate and the non-detrital flux of Co

We solved the sedimentation rate equation (equation (2)) in two different ways (Table S1). We first solved for S in equation (2) using published values of K. To our knowledge, there are only five published values (from only two research groups) of "hydrogenous" or "authigenic" Co fluxes to pelagic clay. These values are 1990 μg/cm^2/Myr [*Zhou and Kyte*, 1992], 2320 and 2490 μg/cm^2/Myr [*Kyte et al*., 1993], as well as 2300 and 5000 μg/cm^2/Myr [*Krishnaswami*, 1976]. Of the five values determined for pelagic clay, the second flux of 5000 μg/cm^2/Myr by *Krishnaswami* [1976] is only briefly mentioned by these authors as it is based on "revised" sedimentation rates, and is regarded as an outlier.

While we cannot apply the Co-based ferromanganese crust and nodule growth rate equations to marine sediment, the flux of non-detrital Co estimated from crusts and nodules is comparable to estimates determined from marine sediment. Non-detrital Co flux to ferromanganese deposits (not sediment) is 2950 μg/cm^2/Myr [*Halbach et al*., 1983] and this value is commonly used in Co-based chronologies applied to nodules and crust. However, *Halbach et al*. [1983] used an approximate average in situ density of 1.6 g/cm^3 in their calculation of K; when corrected to a recent, more refined estimate of average dry bulk density for ferromanganese crust and nodules (1.3 g/cm^3) [*Hein and Koschinsky*, 2014], their data produce a K of 2370 μg/cm^2/Myr, which is comparable to the estimates of K in pelagic sediment. *Frank et al*. [1999] analyzed ferromanganese crusts with lower Co concentrations than those in *Halbach et al*. [1983] and estimated the flux of non-detrital Co to the seafloor to be 1900 μg/cm^2/Myr, which is also within the range estimated from marine sediment. The similarity between the rates at which marine sediment, crusts, and nodules incorporate Co from the water column may suggest a common pathway of Co removal from the water column. Collectively, therefore, we summarize the existing estimates of K from the literature and this study to be between $\sim$1650 and $\sim$2350 μg/cm^2/Myr.

In the second method, we calculate a K value using our own Co data. The calculation of the non-detrital Co flux to the seafloor requires at least two independently determined sediment ages that can be used as boundary conditions to constrain the model. These ages ideally bracket many or all of the sediment samples and establish the time parameter for the rate calculation. At Sites U1366 and U1369, we used the age of the seafloor (0 Ma) and the age of the basement basalt as constraints. IODP Site U1365 is a redrill of DSDP Hole 596 and has matching solid-phase chemical concentration profiles, provided that Site U1365 depths are shifted upward by 2 m (Figure 3). Accordingly, we transferred the K-Pg boundary identified in Hole 596 [*Zhou and Kyte*, 1992] to Site U1365 to act as an age constraint. Other age constraints in Hole 596 [*Zhou and Kyte*, 1992] acted as independent checks. For Site U1370, the constraints are the seafloor and the top of the thin carbonate layer that was dated to be within a few million years of the K-Pg boundary, 65.5 Ma [*D'Hondt et al*., 2011; *Alvarez-Zarikian*, 2015]. We did not extend the calculation of K deeper than the K-Pg boundary at Sites U1365 and U1370 due to the presence of biogenic sediment (chert and carbonates, respectively) to which application of the Co-based method is not appropriate.

For each site each with its own age constraints, for sample *i*,

$$\frac{\Sigma\left(\Delta d_i \times Co_{non\text{-}det..i} \times \rho_i\right)}{\Delta t_t} = K \tag{3}$$

where

Δd_i = hole depth interval that sample i represents (cm);
$Co_{non\text{-}det..i}$ = concentration of non-detrital Co (μg/g);
ρ_i = Dry Bulk Density (g/cm^3);
Δt_t = time in total interval bracketed by age constraints (Myr);
K = non-detrital input rate (μg/cm^2/Myr).

The depth intervals in a hole should sum to equal the total depth of the hole that is bounded on either side by the age constraints.

$$\Sigma\, \Delta d_i = d_t \tag{4}$$

where

d_t = total depth included between age constraints (cm).

If the calculated non-detrital Co flux matches the estimates published in previous literature, these two approaches to the Co-based model should produce similar sedimentation rates and ages for each sample. A different calculated non-detrital Co flux may indicate (1) uncertainty within the parameters or assumptions of the model, or (2) that the previously published values of K are incorrect.

5.3. Ages: Sample-by-Sample

Once instantaneous sedimentation rates are calculated for each sample using both techniques, we calculate the age of the samples (Table S1). Broadly, this is done by applying a series of single instantaneous sedimentation rates to the series of depth segments through the sedimentary sequence (Figure S1). It is critical that the sampling resolution is high enough to capture the compositional variability of the sequence so each sample is an accurate representation of that segment of core.

The age of the shallowest sample can be calculated by applying the instantaneous sedimentation rate of that sample to the depth interval between the younger age constraint and that sample.

$$A_1 = A_0 + \frac{D_1 - D_0}{S_1} \tag{5}$$

where initially $A_0 = 0$ and $D_0 = 0$ if the seafloor is the younger age constraint and

A_1 = age of the shallowest sample (Myr);
D_1 = depth of shallowest sample (cm);
S_1 = instantaneous sedimentation rate of shallowest sample (cm/Myr).

The equation assumes that the sediment within the depth interval between the younger boundary constraint and the shallowest sample accumulated at the instantaneous sedimentation rate that was calculated for the shallowest sample. To calculate the age of the deeper samples, we assume half of the depth interval in between samples has the instantaneous sedimentation rate of the adjacent shallower sample and half of the depth interval has the rate of the adjacent deeper sample (Figure S1). Using the two instantaneous sedimentation rates, we can calculate how much time has passed in between the two samples and add that to the age of the shallower sample to acquire the age of the deeper sample. In this way, samples deeper than the shallowest sample are calculated successively as follows,

$$A_i = A_{i-1} + \frac{\frac{1}{2}(D_i - D_{i-1})}{S_{i-1}} + \frac{\frac{1}{2}(D_i - D_{i-1})}{S_i} \tag{6}$$

A_i = age of the sample (Myr);
D_i = depth of sample (cm);
S_i = instantaneous sedimentation rate of sample (cm/Myr).

The model can estimate the age of the lower boundary constraint (e.g., basalt) by applying the sedimentation rate of the deepest sample to the depth interval between the deepest sample and the lower boundary constraint.

$$A_B = A_n + \frac{(D_B - D_n)}{S_n} \tag{7}$$

A_B = age of lower age constraint (Myr);
A_n = age of deepest sample (Myr);
D_B = depth of lower age constraint (cm);
D_n = depth of deepest sample (cm);
S_n = instantaneous sedimentation rate of deepest sample (cm/Myr).

6. Dating Samples Below the Chert Layer at Site U1365

At Site U1365, the age model cannot be extended continuously from seafloor to the basement basalt because the Co-based method cannot be applied to the ~18 m of chert present from ~44 to 62 mbsf. However, we can create a second age model that calculates ages from basalt and extends stratigraphically upward to the bottom of the chert layer. This technique allows us to calculate ages for samples deeper than the chert layer. We calculate instantaneous sedimentation rates of each sample, S_i, in the same way as described above using equation (2). We used modified versions of equations (5–7) to calculate ages starting with the basement. Using the same notation as equation (7), we determined the age of the deepest sample, n, by:

$$A_n = A_B - \frac{(D_B - D_n)}{S_n} \tag{8}$$

We calculated ages of the samples shallower than the deepest sample using a modified version of equation (6). Using the same notation as equation (6), the calculation is expressed as:

$$A_i = A_{i+1} - \frac{\frac{1}{2}(D_{i+1} - D_i)}{S_{i+1}} - \frac{\frac{1}{2}(D_{i+1} - D_i)}{S_i} \tag{9}$$

where sample $i+1$ refers to the next deepest sample from sample i in the stratigraphic column. By combining this model starting at the basalt with the model starting at the seafloor at Site U1365 (and thus stratigraphically converging toward the thick chert sequence from above and below), we produce an age model for samples above and below the chert layer without applying the Co-based dating method directly to the chert layer itself.

7. Model Uncertainties

Here we sequentially discuss the sensitivity and variability in model outcomes produced by the uncertainties associated with each input parameter. A final determination of uncertainty is not as simple as a standard calculation of error propagation that does not consider error covariance, since many of the uncertainties are related to each other and/or act to cancel each other. Nonetheless, it is illuminating to examine each step in the process of determining a Co-based age model to identify where further improvements can be found.

First, the analysis of Co_t in equation (1) by ICP-MS is precise to ~2% of the measured value [*Dunlea et al.*, 2015], establishing a baseline uncertainty of the entire methodology.

Second, we examine the uncertainty associated with the statistical modeling of the bulk sedimentary composition, from which Co_d in equation (1) is determined. We statistically model the bulk sedimentary

composition to determine the amount of "upper crust," volcanic ash (a rhyolite), apatite, excess silica, Fe-Mn oxyhydroxide, and altered basalt, on a per sample basis [*Dunlea et al*., 2015]. We determine that this number of components (6) and these specific compositions are necessary to fit the multivariate linear modeling. During the multivariate statistical partitioning process described in *Dunlea et al*. [2015], we test different specific compositions for each end-member to check the sensitivity of the partitioning calculations. For example, we test three different rhyolite compositions (e.g., we compare an average rhyolite composition to two discrete ash layers from SPG marine sediment, etc.). Twelve combinations of the six final end-members produce strongly similar trends and fit the dataset equally well. Because there is no reason to favor one model over the rest, we average the modeled mass fraction of each end-member of each sample that is output by the twelve models (e.g., we average the rhyolite results from the 12 models together for each sample, etc.). However, exactly which end-member we use for each of these components matters little for the Co-based accumulation rates. When we separately use the twelve multivariate statistical models [that we average to produce the final compositional model [*Dunlea et al*., 2015]] in the Co-based accumulation rate calculations, they yield non-detrital Co fluxes that varied less than 0.5% from each other. Thus, the potential uncertainty in partitioning end-members with the statistical model has a minimal effect on our age model.

Third, we examine the uncertainty associated with the determination of the amount of Co in each compositional end-member. Average concentrations of Co concentrations in rhyolite are 10 ± 15 μg/g [*GEOROC*, 2014], and typical continental crust sources (Chinese Loess, NASC, PAAS, GLOSS, UCC) range from 17 to 25 μg/g [*Taylor et al*., 1983; *Gromet et al*., 1984; *Taylor and McLennan*, 1985; *Plank and Langmuir*, 1998; *Rudnick and Gao*, 2003]. Whether we use 17 or 25 μg/g in the Co model for the "upper crust" end-member to calculate the Co_d of equation (1) will have more of an effect on the sites with a higher portion of eolian dust and ash (U1369 and U1370). As a sensitivity test, we compare the non-detrital Co fluxes at each site from the highest and lowest reasonable Co concentrations for each detrital end-member; this comparison indicates a $\sim$7% difference in Sites U1365 and U1366 and a $\sim$15% difference in Sites U1369 and U1370.

Fourth, we examine the lower age constraint provided by the age of the basement (ocean basalt) at Sites U1366 and U1369. Obviously, this has a significant impact on age model outcomes when the basement age itself is only broadly known. For example, the basement of Site U1366 occurs within magnetic polarity Chron 34n, which ranges in age from 84 to 124.6 Myr [*D'Hondt et al*., 2011]. Taken at face value, this range causes a 33% difference in the calculated flux of non-detrital Co. However, tectonic models of the complex triple junction where this basement was formed significantly narrows basement age to be within 90–105 Ma [*Pockalny and Dahn*, 2013] and causes only a 14% difference in the flux of non-detrital Co estimates. We selected a mid-point basement age of 95 Ma to construct the model at Site U1366. Although Site U1365 occurs on the same magnetic polarity chron as Site U1366, Re and Os isotope dating of basalt at Site U1365 tightly constrains the basement age to be $\sim$103 Ma (G. L. Zhang, personal communication, 2014). Site U1369 is located within magnetic polarity Chron 25r [*D'Hondt et al*., 2011], which has a narrow basement age range (57.2 to 58.4 Myr) [*Gradstein et al*., 2004] that only causes an $\sim$2% difference in the calculated non-detrital Co flux. At Site U1370 and the shallower interval (0–18 mbsf) of Site U1365, the K-Pg boundary is used as the lower age constraint and has a well-known age with essentially zero uncertainty [*Zhou and Kyte*, 1992; *Alvarez-Zarikian*, 2015].

Fifth, the model would be improved with a more rigorous stratigraphic correlation at each site. If samples in this study from different holes at a single site do not correctly overlap, they will not represent an accurate interval of sediment. Additionally, core gaps that align between different holes at the same site prevent the construction of a complete splice and some of the total sediment depth may be missing. When calculating the non-detrital Co input rate, K (equation (2)), a missing segment of core would lower the total sum of non-detrital Co that accumulated between the age brackets causing the overall K to be too low.

Sixth, ash layers, hardgrounds, hiatuses, intervals of rapid biogenic deposition, or other instances of either very high or very low sedimentation rate can impose error on the age model by introducing depth intervals that are not representative of the rest of the sequence. For example, if a bulk sample is used to represent an interval that includes a discrete ash layer or if a bulk sample included part of an altered discrete ash layer, the samples will not represent the overall sediment composition. To account for hardgrounds in the sediment column when developing their estimates of non-detrital Co, *Zhou and Kyte* [1992] used a Mn-encrusted hardground thickness and average composition to calculate the amount of extra "hydrogenous"

Co incorporated into this phase (stated to be 5% more Co) and added it to the total "hydrogenous" Co. This value is untestable and we do not include any such approximations. At Site U1365, we were able to date samples shallower and deeper than the anomalous chert layer by combining two age models, one starting from the seafloor and going to the K-Pg boundary and the second starting from the basalt and extending up to the bottom of the chert layer, as described above. At Site U1370, core disturbance (flow-in) and our small number of samples below the carbonate layer prevented us from modeling the age of sediment below the K-Pg boundary.

The above presentation highlights the importance of understanding uncertainty *at each site* in a Co-based age model, due to the fact that each site is likely to have a unique set of conditions and/or assumptions associated with it. Some of the uncertainties introduce systematic errors and others introduce random errors that propagate differently. To arrive at a final general confidence level for each age model, we have taken the approach of running "ensembles" of models that allow us to collectively assess variability in the final result at any given site.

8. Non-detrital Co Fluxes at Sites U1365, U1366, U1369, and U1370

Analyses, calculations, and models from Sites U1366 and U1369 separately produce a flux of non-detrital Co (1812 and 1652 $\mu g/cm^2$/Myr, respectively) that is close to, but slightly less than, the lowest previously published estimate for pelagic clay of 1990 $\mu g/cm^2$/Myr [*Zhou and Kyte*, 1992].

For Site U1365, using the K-Pg boundary as a lower age constraint, the modeling yields a non-detrital Co flux of 2051 $\mu g/cm^2$/Myr. This is very close to the value of 1990 $\mu g/cm^2$/Myr for nearby Hole 596 by *Zhou and Kyte* [1992], despite minor differences in approach.

Site U1370 produced a non-detrital Co flux of 4176 $\mu g/cm^2$/Myr, which is the highest value amongst the SPG sites, but still lower than the highest previously published estimates of 5000 $\mu g/cm^2$/Myr [*Krishnaswami*, 1976]. However, considering the tight clustering of other previously published values and estimates in this study from Sites U1366, U1369, and U1365 (to the K-Pg boundary), we believe our Site U1370 estimate is not representative of regional fluxes. Instead, as discussed later in this paper, we regard this estimate of K at Site U1370 to reflect a local increase due to an enhanced source of Co affecting Co concentrations in the overlying water.

We estimate the non-detrital flux of Co to pelagic clay ranges from 2000 ± 350 $\mu g/cm^2$/Myr and use this range of K values in our model to further assess the sensitivity of Co-based ages and sedimentation rates at each site (Table S1 and Figures 4 and 5). Because instantaneous sedimentation rates are directly proportional to K, rates produced using a K of 1650 $\mu g/cm^2$/Myr are 30% different than rates produced with a K of 2350 $\mu g/cm^2$/Myr (since the two K values are 30% different). Unlike sedimentation rates, age estimates from different K values become more divergent as time intervals between independent age constraints lengthen. Because flux estimates are rates, the difference in ages produced by these two K values increases with time. Thus, Site U1366 with a basement age of $\sim$95 Ma exhibits up to a 31 Myr difference between the models with two different K values, while Site U1369 with a basement age of 58 Ma exhibits a 17 Myr difference.

As per equations (2) and (5)–(7), the non-detrital Co at each site also influences estimates of sedimentation rate and age. Higher fluxes of non-detrital Co (e.g., Site U1370) amplify the resultant K value, producing a more divergent age model than a site with lower fluxes of non-detrital Co (e.g., U1365). Consequently, although we modeled the same time interval (0–65.5 Ma) at Sites U1365 and U1370, the two K values produced ages that differed more at Site U1370 (49 Myr) than at Site U1365 (24 Myr). This is because the higher non-detrital flux of Co that we calculated at Site U1370 relative to Site U1365 translates into very slow sedimentation rates and thus a greater difference in age estimates at Site U1370.

In summary, at each site, the sensitivity of modeled ages to varying non-detrital Co fluxes is controlled mainly by the length of the time interval between independent age boundary constraints and the fluxes of non-detrital Co. In our interpretations, we consider the models created using the range of K values as part of our ensemble approach. Additional independent discrete age points would reduce the uncertainty in age estimates caused by variability in non-detrital Co flux.

We do not have access to additional independent age constraints at Sites U1366, U1369, or U1370. However, independent age constraints from Hole 596 that were depth shifted upward by 2 m at Site U1365

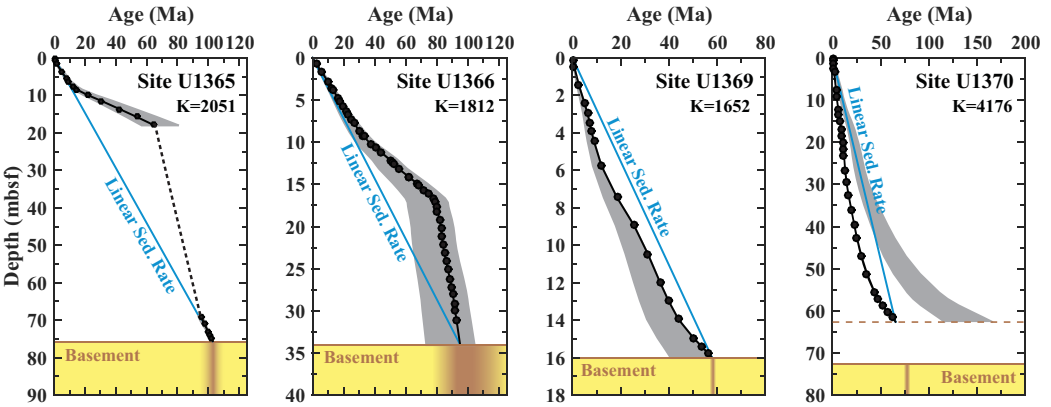

Figure 4. Age (Ma) versus depth (mbsf) at the four SPG sites. The black dots are the Co-based models for each site that were analyzed using the non-detrital Co flux calculated from the Co data and age constraints specific to that site (K in $\mu g/cm^2/Myr$). The maximum and the minimum non-detrital Co flux (2350 and 1650 $\mu g/cm^2/Myr$) estimates were also analyzed in each model to determine uncertainty in the ages (shaded gray area). For comparison, an age model constructed assuming a simple linear sedimentation rate from the seafloor to the basement (or to the K-Pg boundary at Site U1370) is plotted (blue line). Site U1365 is a combination of two Co-based models, one beginning from the seafloor and a second beginning from the basement, to avoid application of the Co-based model to the interval of chert (~44 to 62 mbsf). The sediment-basalt interface is marked by a solid brown line and below is shaded in yellow with the darker gradient depicting the uncertainty in basement age. At Site U1370, a brown dashed line marks the K-Pg boundary that was used as a lower age constraint for the calculations of K at that site.

(Figure 3) indicate that the ages produced in this study agree within 7 Myr. Given the uncertainties of the model (section 6), these estimated ages are consistent with the independent age checks within error. Compared with the assumptions and results of the linear sedimentation rate model, our Co-based model significantly improves age and sedimentation rate estimates at every site we studied (Figures 4 and 5).

9. How Constant is the Flux of Non-detrital Co to Pelagic Clay?

The historical development and application of Co-based accumulation rate modeling has implicitly or explicitly (depending on the study) considered that the flux of non-detrital Co to the seafloor is spatially and temporally constant, at least within the uncertainty imposed by the range of input parameters. While additional age constraints are required to define temporal variations within a site, our multi-site approach shows that there are spatial differences in non-detrital Co flux to the seafloor throughout the SPG.

Our non-detrital Co fluxes from Sites U1366 and U1369 are slightly lower than previously published global values. The earlier values are from sites in the North Pacific or closer to continents in the SPG. In contrast, plate reconstructions of Sites U1366 and U1369 indicate that they have always been located toward the center of the SPG (Figure 1). Gyre centers have lower Co concentrations in seawater, which we infer caused the lower non-detrital Co flux results at these two sites. Additionally, extremely low levels of productivity near the center of the gyre would minimize any potential biological export of Co to the seafloor. Such variations in the water column are key to understanding the spatial and temporal variability of Co fluxes to the seafloor.

Site U1370 was located relatively close to Antarctica (~800 km) [*Gurnis et al*., 2012] at the beginning of the Cenozoic (~65 Ma), a time when ocean circulation patterns were very different from today. Indeed, with the Drake Passage and Tasmanian Gateway then closed [*Barker et al*., 2007], some ocean models predict a second polar gyre that circulated in the region where Site U1370 was located at the time [*Huber et al*., 2004]. These paleoceanographic conditions, along with proximity to Antarctica, could have increased the non-detrital flux to Site U1370 in a variety of ways, including: (i) OMZ expansion/contraction causing higher Co concentrations in the overlying water column, (ii) upwelling along the gyre boundaries causing redistribution of Co and other nutrients, and (iii) increased biogenic export of Co to the seafloor in regions of enhanced upwelling. While we are unable to differentiate the relative importance of these processes in the past, even at the present-day Site U1370 remains further southeast and closer to continents than Sites U1366 and U1369 (Figure 1). Consequently, it may still receive a higher flux of non-detrital Co. This proximity to continents, and the associated oceanographic variables mentioned above, may lead to higher

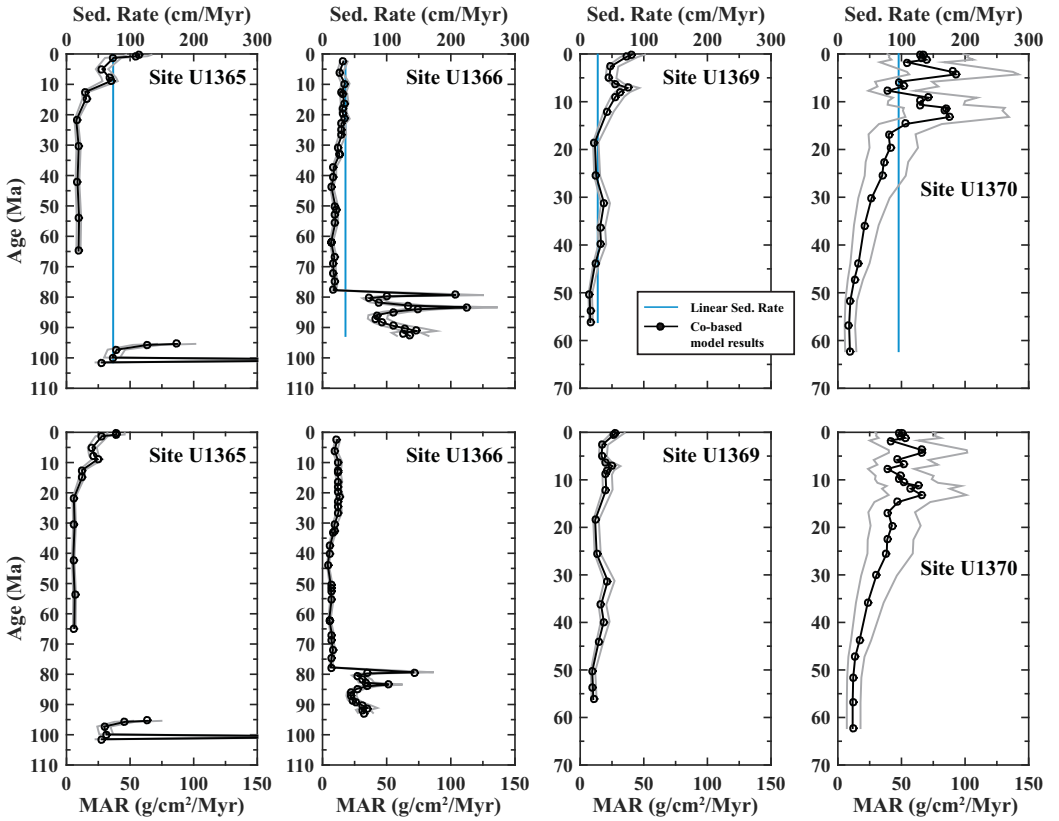

Figure 5. (top row) Instantaneous sedimentation rate (cm/Myr) versus age (Ma). (bottom row) Bulk sediment mass accumulation rate (g/cm^2/Myr) versus age (Ma). Ages are modeled with the non-detrital Co flux estimates specific to each site. Instantaneous sedimentation rates are an average of three models using a non-detrital flux estimate of 1650 μg/cm^2/Myr, 2350 μg/cm^2/Myr, and the estimate calculated specific to each site. The gray lines represent the maximum and minimum in these ranges. The simple linear sedimentation rate (from Figure 4) is plotted for comparison (blue lines). The gap in the Co-based model at Site U1365 contains the chert layer to which the Co-based technique cannot be directly applied.

amounts of Co in the water column and result in the higher non-detrital flux to the seafloor. This would explain the high K values we determined for Site U1370.

Since the processes that affect non-detrital Co removal to the seafloor may be more variable close to continents and in regions of upwelling, a Co-based age model is most effective in open ocean regions far from shore, where the concentration of Co in the water column is relatively homogenous. The relative homogeneity of Co concentrations in the open ocean and the slow, leaky process by which Co is deposited to the seafloor cause it to be inversely proportional to sedimentation rate. Co-based age models are best suited at locations where the sediments remain completely oxygenated [*Fischer et al*., 2009; *D'Hondt et al*., 2011, 2015; *Røy et al*., 2012]. Nearer to continents, seawater heterogeneities and potential long-term variations in OMZ strength and extent, upwelling, and biogenic export of Co decrease the applicability of Co-based age models. Certainly, comparing proximal and distal locations is not advised, due to these known variations in seawater chemistry and removal process.

Co-based age models applied to shorter, more recent time scales are likely to be more accurate given the similarities between the present day and the past distribution of Co in the water column and flux of non-detrital Co to the seafloor. To apply a Co-based age model to longer time scales requires consideration of the paleolocation of the given site and awareness that the Co distribution in the water column may have changed over time in ways that are unknown. Additional independent age constraints (from Os isotope or Sr isotope analyses) could be used to track the temporal variability of the non-detrital Co flux to the seafloor by bracketing different time intervals covered in the sedimentary sequence. A Co-based model constrained with independent ages that is carefully applied to the appropriate site or intervals within a site is capable of providing an effective record of sedimentation rates and ages of pelagic clay.

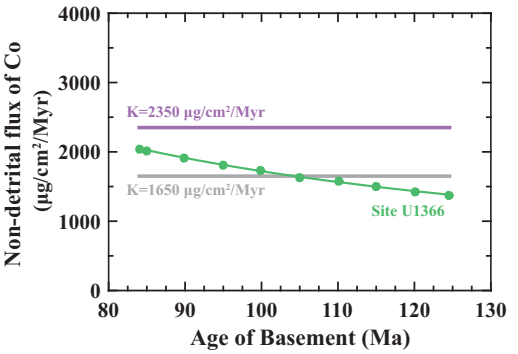

Figure 6. Estimates of the flux of non-detrital Co at Site U1366 (green dots) that are calculated using the range of basement ages inferred from the magnetic polarity Chron 34n (84–124.6 Ma) [*Gradstein et al.*, 2004]. Site U1366 only produces non-detrital Co fluxes within the range of current estimates (1650–2350 μg/cm^2/Myr) when the basement age is 84–104 Ma.

10. How Fast Did the Chert Accumulate at Site U1365?

Although the Co-based method is not directly applicable to the chert layer at Site U1365, it can be used indirectly to estimate how quickly the chert and surrounding Si-rich sediment accumulated. At Site U1365, we constructed two Co-based age models, one starting from the seafloor and extending downward to the K-Pg boundary and the other starting at the basalt and extending upward to the base of the chert layer. According to the Co-based age models, the 50.9 m gap occurred in 30.5 Myr, suggesting that the average sedimentation rate of the chert and clay with excess Si was 1.67 m/Myr (0.167 cm/kyr). Since the interval between the Co-based models at Site U1365 includes both chert and pelagic clay interlaced with porcellanite layers, it is likely that the accumulation rate was not constant over this entire interval, but slower during the accumulation of clay and faster during chert accumulation. Regardless, our estimate of chert accumulation is an improvement over simple linear sedimentation rate estimates derived from the age of the seafloor and basalt.

11. Improving Basement Age Constraints at Site U1366

In addition to dating pelagic clay, the Co-based model can be a powerful tool for constraining basement age ranges. For example, Site U1366 was formed in a tectonically complex region and its basement age is difficult to tectonically model any more tightly than the range of ages determined by the magnetic polarity chron (84–124.6 Ma). Using this range of basement ages in the Co-based model produces a range of non-detrital Co-fluxes, some of which are comparable to the current estimates of K (2000 ± 350 μg/cm^2/Myr) and some of which are lower (Figure 6). Calculation of non-detrital Co flux estimates that are lower than the current known range of K (<1650 μg/cm^2/Myr) suggests that a basement age estimate is too high. At Site U1366, non-detrital Co fluxes within the range of known estimates only occur when using ages that range from 85 to 104 Ma. This range is narrower than the range given by the magnetic polarity chron and agrees with additional tectonic modeling of abyssal hill lineations in the region that estimate basement age to be 90–105 Ma [*Pockalny and Dahn*, 2013].

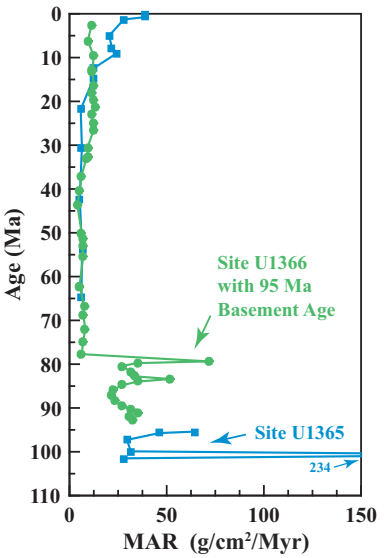

Figure 7. Bulk sediment mass accumulation rate (g/cm^2/Myr) versus age (Ma) for Sites U1365 and U1366 (from Figure 5) are plotted using basement ages of 95 and 103 Ma, respectively. The double peaks at both sites are likely not synchronous.

12. Are the Double Peaks at Sites U1365 and U1366 Synchronous?

Our results indicate that two local maxima in sedimentation rate occurred near the basement at both Sites U1365 and U1366, which are located relatively near each other (Figure 7). It is possible that these were synchronous events recorded at both sites. However, to align these double peaks, the basement at Site U1366 would have to be 115 Ma, and the non-detrital Co would have accumulated with a K value of 1497 μg/cm^2/Myr. While 115 Ma is within the basement age range defined by the magnetic polarity chron, it is clearly higher than more refined tectonic modeling predicts [*Pockalny and Dahn*, 2013]. Furthermore, the K value of $\sim$1500 μg/cm^2/Myr is lower than our determined accepted range (Figure 6). Thus, it is unlikely that the two deep local maxima were synchronous at Sites U1365 and U1366. Instead, hydrothermal, biogenic Si, and ash layer deposits identified in these intervals may be responsible for the high and variable sedimentation rates [*Dunlea et al.*, 2015].

13. Conclusion

Our basin-wide, multi-site approach highlights the utility of Co-based age models for quantitative, stratigraphically useful, age control in otherwise homogeneous ultra-fine grained pelagic clay sequences. Furthermore, we are able to assess variability in the flux of non-detrital Co to pelagic clay and relate it to Co concentration heterogeneities within the water column. The accumulation rate of non-detrital Co is not "constant." After addressing the variable deposition of non-detrital Co, we have identified a series of conditions that must be met for this dating method to work at a given location and successfully constructed age models to 65.5, 95, and 58 Ma, for SPG Sites U1365, U1366, and U1369, respectively. We also apply this Co-based technique to improve estimates of chert accumulation at Site U1365, and help constrain loosely defined basement ages at Site U1366 and thus support tectonic modeling results.

A site is ideally suited for a Co-based age model if it has always been completely oxygenated and located in the distal open ocean since being created at a MOR. Sites nearer to continents in the present or past are more susceptible to heterogeneities in seawater composition and potential long-term variations in OMZ strength and extent and biological export of Co; these susceptibilities decrease the applicability of Co-based age models for such locations. For example, we show that Site U1370 received an anomalously high flux of non-detrital Co, most likely because it was too close to a source of Co to the water column from sediment along the coast of Antarctica at the beginning of the Cenozoic.

We estimate the non-detrital Co flux to pelagic clay in the open ocean to be 2000 $\pm$ 350 μg/cm^2/Myr. Deviations from this range may indicate variable non-detrital Co deposition, poorly constrained independent ages, and/or the presence of an anomalous sediment layer or hiatus.

We used the Co-based technique as a method to determine instantaneous sedimentation rate in sequences with virtually no other age control. However, the Co-based technique could be inverted to examine temporal changes in the water column. For example, future Co work at a site with excellent independent age control, could track variations in non-detrital Co deposition during different time intervals of sediment deposition. Combined with the paleoposition of the site, these variations in Co accumulation could provide insight into large-scale alteration and redox state of coastal sediment and OMZ behavior throughout the Cenozoic.

Acknowledgments

We thank B. Peucker-Ehrenbrink, M. Frank, and an anonymous reviewer for their terrific comments on the manuscript. We are grateful to T. Ireland, J. W. Sparks, and R. P. Scudder at Boston University for their analytical assistance and many conversations. We also greatly appreciate the help of C. Atta and M. Hulewicz in the lab. We thank G. L. Zhang for allowing us to use his basement age at Site U1365 to constrain our model. We are also very grateful to M. A. Saito and N. Hawco for their interesting conversations about cobalt. This research used samples and data provided by the Integrated Ocean Drilling Program (IODP). Funding for this research was provided by the U.S. National Science Foundation (OCE1130531 to R. W. Murray and OCE1130735 to S. D'Hondt and A. J. Spivack) and USSSP postcruise support to Expedition 329 shipboard participants R.W. Murray, R. N. Harris, S. D'Hondt, and A. J. Spivack. Portions of this material are based on work supported while R.W.M. was serving at the National Science Foundation.

References

Alvarez-Zarikian, C. A. (2015), Cenozoic bathyal and abyssal ostracods beneath the oligotrophic South Pacific Gyre (IODP Expedition 329 Sites U1367, U1368 and U1370), *Palaeogeogr. Palaeoclimatol. Palaeoecol.*, *419*, 115–142.

Aparicio-González, A., C. M. Duarte, and A. Tovar-Sánchez (2012), Trace metals in deep ocean waters: A review, *J. Mar. Syst.*, *100-101*, 26–33.

Backman, J., et al. (2008), Age model and core-seismic integration for the Cenozoic Arctic Coring Expedition sedimenets from the Lomonosov Ridge, *Paleoceanography*, *23*, PA1S03, doi:10.1029/2007PA001476.

Banakar, V. K., J. N. Pattan, and A. V. Mudholkar (1997), Palaeoceanographic conditions during the formation of a ferromanganese crust from the Afanasiy-Nikitin seamount, North Central Indian Ocean: Geochemical evidence, *Mar. Geol.*, *136*, 299–315.

Barker, P. F., G. M. Filippelli, F. Florindo, E. E. Martin, and H. D. Scher (2007), Onset and role of the Antarctic Circumpolar Current, *Deep Sea Res., Part II*, *54*, 2388–2398.

Bourles, D., G. M. Raisbeck, and F. Yiou (1989), ^{10}Be and ^{9}Be in marine sediments and their potential for dating, *Geochim. Cosmochim. Acta*, *53*, 443–452.

Bown J., M. Boye, A. Baker, E. Duvieilbourg, F. Lacan, F. Le Moigne, F. Planchon, S. Speich, and D. M. Nelson (2011), The biogeochemical cycle of dissolved cobalt in the Atlantic and the Southern Ocean south off the coast of South Africa, *Mar. Chem.*, *126*, 193–206.

Castrillejo, M., P. J. Statham, G. R. Fones, H. Planquette, F. Idrus, and K. Roberts (2013), Dissolved trace metals (Ni, Zn, Co, Cd, Pb, Al, and Mn) around the Crozet Islands, Southern Ocean, *J. Geophys. Res. Oceans*, *118*, 1–14, doi:10.1002/jgrc.20359.

Cowen, J. P., and K. W. Bruland (1985), Metal deposits associated with bacteria: Implications for Fe and Mn marine biogeochemistry, *Deep Sea Res., Part A*, *32*, 253–272.

Dalai, T. K., and G. Ravizza (2006), Evaluation of osmium isotopes and iridium as paleoflux tracers in pelagic carbonates, *Geochim. Cosmochim. Acta*, *70*, 3928–3942.

D'Hondt, S., et al. (2009), Subseafloor sedimentary life in the South Pacific Gyre, *Proc. Natl. Acad. Sci. U. S. A.*, *106*, 11,651–11,656.

D'Hondt, S., F. Inagaki, C. A. Alvarez Zarikian, and Expedition 329 Scientists (2011), *Proceedings of the Integrated Ocean Drilling Program*, vol. 329, Integrated Ocean Drill. Program Manage. Int. Inc., Tokyo, doi:10.2204/iodp.proc.329.2011.

D'Hondt, S., et al. (2015), Presence of oxygen and aerobic communities from sea floor to basement in deep-sea sediments, *Nat. Geosci.*, *8*, 299–304.

Dulaquais, G., M. Boye, and R. Middag (2014a), Contrasting biogeochemical cycles of cobalt in the surface Western Atlantic Ocean, *Global Biogeochem. Cycles*, *28*, 1–26, doi:10.1002/2014GB004903.

Dulaquais, G., M. Boye, M. J. A. Rijkenberg, and X. Carton (2014b), Physical and remineralization processes govern the cobalt distribution in the deep western Atlantic Ocean, *Biogeosciences*, *11*, 1561–1580.

Dunlea, A. G., R. W. Murray, J. Sauvage, A. J. Spivack, R. N. Harris, and S. D'Hondt (2015), Dust, volcanic ash, and the evolution of the South Pacific Gyre through the Cenozoic, *Paleoceanography*, doi:10.1002/2015PA002829, in press.

Farley, K. A. (1995), Cenozoic variations in the flux of interplanetary dust recorded by He-3 in a deep-sea sediment, *Nature*, *376*, 153–156.

Farley, K. A., A. Montanari, and R. Coccioni (2012), A record of the extraterrestrial 3He flux through the Late Cretaceous, *Geochim. Cosmochim. Acta*, *84*, 314–328.
Fischer, J. P., T. G. Ferdelman, S. D'Hondt, H. Røy, and F. Wenzhöfer (2009), Oxygen penetration deep into the sediment of the South Pacific gyre, *Biogeosciences*, *6*, 1467–1478.
Frank, M., R. K. O'Nions, J. R. Hein, and V. K. Banakar (1999), 60 Myr records of major elements and Pb–Nd isotopes from hydrogenous ferromanganese crusts: Reconstruction of seawater paleochemistry, *Geochim. Cosmochim. Acta*, *63*, 1689–1708.
Frank M., J. Backman, M. Jakobsson, K. Moran, M. O'Regan, J. King, B. A. Haley, P. W. Kubik, and D. Garbe-Schönberg (2008), Beryllium isotopes in central Arctic Ocean sediments over the past 12.3 million years: Stratigraphic and paleoclimatic implications, *Paleoceanography*, *23*, PA1S02, doi:10.1029/2007PA001478.
Gale, A., C. A. Dalton, C. H. Langmuir, Y. Su, and J.-G. Schilling (2013), The mean composition of ocean ridge basalts, *Geochem. Geophys. Geosyst.*, *14*, 489–518, doi:10.1029/2012GC004334.
GEOROC (2014), *Geochemistry of Rocks of the Oceans and Continents*, Max Planck Institute for Chemistry Mainz, Germany. [Available at http://georoc.mpch-mainz.gwdg.de/georoc/.]
German, C., G. Klinkhammer, J. Edmond, A. Mitra, and H. Elderfield (1990), Hydrothermal scavenging of rare-earth elements in the ocean, *Nature*, *345*, 516–518.
Gleason, J. D., T. C. Moore, D. K. Rea, T. M. Johnson, R. M. Owen, J. D. Blum, S. A. Hovan, and C. E. Jones (2002), Ichthyolith strontium isotope stratigraphy of a Neogene red clay sequence: Calibrating eolian dust accumulation rates in the central North Pacific, *Earth Planet. Sci. Lett.*, *202*, 625–636.
Gradstein, F. M., J. G. Ogg, and A. G. Smith (Eds.) (2004), *A Geologic Time Scale 2004*, 610 pp., Cambridge Univ. Press, Cambridge, U. K.
Gromet, L. P., R. F. Dymek, L. A. Haskin, and R. L. Korotev (1984), The "North American shale composite": Its compilation, major and trace element characateristics, *Geochim. Cosmochim. Acta*, *48*, 2469–2482.
Gurnis, M., M. Turner, S. Zahirovic, L. DiCaprio, S. Spasojevic, R. D. Müller, J. Boyden, M. Seton, V. C. Manea, and D. J. Bower (2012), Plate tectonic reconstructions with continuously closing plates, *Comput. Geosci.*, *38*, 35–42.
Halbach, P., R. Giovanoli, and D. Borstel Von (1982), Geochemical processes controlling the relationship between Co, Mn, and Fe in early diagenetic deep-sea nodules, *Earth Planet. Sci. Lett.*, *60*, 226–236.
Halbach, P., M. Segl, D. Puteanus, and A. Mangini (1983), Co-fluxes and growth-rates in ferromanganese deposits from central Pacific Seamount Areas, *Nature*, *304*, 716–719.
Heath, G. R., and J. Dymond (1977), Genesis and transformation of metalliferous sediments from the East Pacific Rise, Bauer Deep, and Central Basin, northwest Nazca plate, *Geol. Soc. Am. Bull.*, *88*, 723–733.
Hein, J. R., and A. Koschinsky (2014), Deep-Ocean Ferromanganese Crusts and Nodules, In *Treatise on Geochemistry (Second Edition)*, edited by H. D. H. K. Turekian, *Treatise on Geochemistry (Second Edition)*, pp. 273–291, Elsevier, Oxford, U. K.
Hein, J. R., T. A. Conrad, M. Frank, M. Christl, and W. W. Sager (2012), Copper-nickel-rich, amalgamated ferromanganese crust-nodule deposits from Shatsky Rise, NW Pacific, *Geochem. Geophys. Geosyst.*, *13*, Q10022, doi:10.1029/2012GC004286.
Huber, M., H. Brinkhuis, C. E. Stickley, K. Doos, A. Sluijs, J. Warnaar, S. A. Schellenberg, and G. L. Williams (2004), Eocene circulation of the Southern Ocean: Was Antarctica kept warm by subtropical waters, *Paleoceanography*, *19*, PA4026, doi:10.1029/2004PA001014.
Ingram, B. L. (1995), High-resolution dating of deep-sea clays using Sr isotopes in fossil fish teeth, *Earth Planet. Sci. Lett.*, *134*, 545–555.
Ireland, T. J., R. P. Scudder, A. G. Dunlea, C. H. Anderson, and R. W. Murray (2014), Assessing the accuracy and precision of inorganic geochemical data produced through flux fusion and acid digestion: Multiple (60+) comprehensive analyses of BHVO-2 and the development of improved "Accepted" values, Abstract V41A-4767 presented at 2014 Fall Meeting, AGU, San Francisco, Calif.
Kadko, D. (1985), Late Cenozoic sedimentation and metal-deposition in the North Pacific, *Geochim. Cosmochim. Acta*, *49*, 651–661.
Klemm, V., S. Levasseur, M. Frank, J. R. Hein, and A. N. Halliday (2005), Osmium isotope stratigraphy of a marine ferromanganese crust, *Earth Planet. Sci. Lett.*, *238*, 42–48.
Knauer, G. A., J. H. Martin, and R. M. Gordon (1982), Cobalt in north-east Pacific waters, *Nature*, *297*, 49–51.
Krishnaswami, S. (1976), Authigenic transition-elements in Pacific Pelagic Clays, *Geochim. Cosmochim. Acta*, *40*, 425–434.
Kyte, F. T., and J. T. Wasson (1986), Accretion rate of extraterrestrial matter: Iridium deposited 33 to 67 million years ago, *Science*, *232*, 1225–1229.
Kyte, F. T., M. Leinen, G. R. Heath, and L. Zhou (1993), Cenozoic sedimentation history of the central North Pacific: Inferences from the elemental geochemistry of core LL44-GPC3, *Geochim. Cosmochim. Acta*, *57*, 1719–1740.
Leinen, M. (1989), The pelagic clay province of the North Pacific Ocean, in *The Geology of North America*, edited by E. L. Winterer, D. M. Hussong, and R. W. Decker, pp. 323–335, Geol. Soc. Am., Boulder, Colo.
Leinen, M., and N. Pisias (1984), An objective technique for determining end-member compositions and for partitioning sediments according to their sources, *Geochim. Cosmochim. Acta*, *48*, 47–62.
Li, J., N. Fang, W. Qu, X. Ding, L. Gao, C. Wu, and Z. Zhang (2008), Os isotope dating and growth hiatuses of Co-rich crust from central Pacific, *Sci. China, Ser. D*, *51*, 1452–1459.
Manheim, F. T., and C. M. Lane-Bostwick (1988), Cobalt in ferromanganese crusts as a monitor of hydrothermal discharge on the Pacific sea floor, *Nature*, *335*, 59–62.
Marcantonio, F., R. F. Anderson, M. Stute, N. Kumar, P. Schlosser, and A. Mix (1996), Extraterrestrial 3He as a tracer of marine sediment transport and accumulation, *Lett. Nat.*, *383*, 705–707.
Martin, E., and B. Haley (2000), Fossil fish teeth as proxies for seawater Sr and Nd isotopes, *Geochim. Cosmochim. Acta*, *64*, 835–847.
McDonough, W. F., and S.-S. Sun (1995), The composition of the Earth, *Chem. Geol.*, *120*, 223–253.
McMurtry, G. M., D. L. VonderHaar, A. Eisenhauer, J. J. Mahoney, and H.-W. Yeh (1994), Cenozoic accumulation history of a Pacific ferromanganese crust, *Earth Planet. Sci. Lett.*, *125*, 105–118.
Miesch, A. (1976), Q-mode factor analysis of compositional data, *Comput. Geosci.*, *1*, 147–159.
Moffett, J. W., and J. Ho (1996), Oxidation of cobalt and manganese in seawater via a common microbially catalyzed pathway, *Geochim. Cosmochim. Acta*, *60*, 3415–3424.
Müller, R. D., M. Sdrolias, C. Gaina, and W. R. Roest (2008), Age, spreading rates, and spreading asymmetry of the world's ocean crust, *Geochem. Geophys. Geosyst.*, *9*, Q04006, doi:10.1029/2007GC001743.
Murray, R., and M. Leinen (1996), Scavenged excess aluminum and its relationship to bulk titanium in biogenic sediment from the central equatorial Pacific Ocean, *Geochim. Cosmochim. Acta*, *60*, 3869–3878.
Murray, R., M. Leinen, and A. Isern (1993), Biogenic flux of Al to sediment in the central equatorial Pacific Ocean: Evidence for increased productivity during glacial periods, *Paleoceanography*, *8*, 651–670.

Murray, R., D. J. Miller, and K. Kryc (2000), Analysis of major and trace elements in rocks, sediments, and interstitial waters by inductively coupled plasma–atomic emission spectrometry (ICP-AES), *Ocean Drill. Program Tech. Note*, *29*, 1–27.
Noble, A. E., M. A. Saito, K. Maiti, and C. R. Benitez-Nelson (2008), Cobalt, manganese, and iron near the Hawaiian Islands: A potential concentrating mechanism for cobalt within a cyclonic eddy and implications for the hybrid-type trace metals, *Deep Sea Res., Part II*, *55*, 1473–1490.
Noble, A. E., et al. (2012), Basin-scale inputs of cobalt, iron, and manganese from the Benguela-Angola front to the South Atlantic Ocean, *Limnol. Oceanogr.*, *57*, 989–1010.
Nolan, C. V., S. W. Fowler, and J.-L. Teyssie (1992), Cobalt speciation and bioavailability in marine organisms, *Mar. Ecol. Prog. Ser.*, *88*, 105–105.
Paquay, F. S., G. Ravizza, and R. Coccioni (2014), The influence of extraterrestrial material on the late Eocene marine Os isotope record, *Geochim. Cosmochim. Acta*, *144*, 238–257.
Pegram, W. J., and K. K. Turekian (1999), The osmium isotopic composition change of Cenozoic sea water as inferred from a deep-sea core corrected for meteoritic contributions, *Geochim. Cosmochim. Acta*, *63*, 4053–4058.
Peucker-Ehrenbrink, B., G. Ravizza, and A. W. Hofmann (1995), The marine $^{187}Os/^{186}Os$ record of the past 80 million years, *Earth Planet. Sci. Lett.*, *130*, 155–167.
Pisias, N. G., R. W. Murray, and R. P. Scudder (2013), Multivariate statistical analysis and partitioning of sedimentary geochemical data sets: General principles and specific MATLAB scripts, *Geochem. Geophys. Geosyst.*, *5*, 1–6, doi:10.1002/ggge.20247.
Plane, J. M. C. (2012), Cosmic dust in the earth's atmosphere, *Chem. Soc. Rev.*, *41*, 6507–6518.
Plank, T., and C. H. Langmuir (1998), The chemical composition of subducting sediment and its consequences for the crust and mantle, *Chem. Geol.*, *145*, 325–394.
Pockalny, R. A., and M. R. Dahn (2013), Tectonic reconstruction models for the break-up and divergence of the Manihiki & Hikurangi plateau, Abstract T51F-2530presented at 2013 Fall Meeting, AGU, San Francisco, Calif.
Puteanus, D., and P. Halbach (1988), Correlation of Co concentration and growth rate—A method for age determination of ferromanganese crusts, *Chem. Geol.*, *69*, 73–85.
Ravizza, G. (2007), Reconstructing the marine 187Os/188Os record and the particulate flux of meteoritic osmium during the late Cretaceous, *Geochim. Cosmochim. Acta*, *71*, 1355–1369.
Rea, D. K., and M. K. Bloomstine (1986), Neogene history of the South Pacific tradewinds: Evidence for hemispherical asymmetry of atmospheric circulation, *Palaeogeogr. Palaeoclimatol. Palaeoecol.*, *55*, 55–64.
Røy, H., J. Kallmeyer, R. R. Adhikari, R. Pockalny, B. B. Jørgensen, and S. D'Hondt (2012), Aerobic microbial respiration in 86-million-year-old deep-sea red clay, *Science*, *336*, 922–925.
Rudnick, R. L., and S. Gao (2003), Composition of the Continental Crust, in *Treatise on Geochemistry*, edited by H. D. H. K. Turekian, Treatise on Geochemistry, pp. 1–64, Pergamon, Oxford, U. K.
Saito, M. A., and J. W. Moffett (2001), Complexation of cobalt by natural organic ligands in the Sargasso Sea as determined by a new high-sensitivity electrochemical cobalt speciation method suitable for open ocean work, *Mar. Chem.*, *75*, 49–68.
Saito, M. A., and J. W. Moffett (2002), Temporal and spatial variability of cobalt in the Atlantic Ocean, *Geochim. Cosmochim. Acta*, *66*, 1943–1953.
Scudder, R. P., R. W. Murray, and T. Plank (2009), Dispersed ash in deeply buried sediment from the northwest Pacific Ocean: An example from the Izu–Bonin arc (ODP Site 1149), *Earth Planet. Sci. Lett.*, *284*, 639–648.
Scudder, R. P., R. W. Murray, J. C. Schindlbeck, S. Kutterolf, F. Hauff, and C. C. McKinley (2014), Regional-scale input of dispersed and discrete volcanic ash to the Izu-Bonin and Mariana subduction zones, *Geochem. Geophys. Geosyst.*, *15*, 4369–4379, doi:10.1002/2014GC005561.
Seton, M., et al. (2012), Global continental and ocean basin reconstructions since 200 Ma, *Earth Sci. Rev.*, *113*, 212–270.
Shelley, R. U., et al. (2012), Controls on dissolved cobalt in surface waters of the Sargasso Sea: Comparisons with iron and aluminum, *Global Biogeochem. Cycles*, *26*, GB2020, doi:10.1029/2011GB004155.
Stancin, A. M., J. D. Gleason, S. A. Hovan, D. K. Rea, R. M. Owen, T. C. Moore Jr, C. M. Hall, and J. D. Blum (2008a), Miocene to recent eolian dust record from the Southwest Pacific Ocean at 40° S latitude, *Palaeogeogr. Palaeoclimatol. Palaeoecol.*, *261*, 218–233.
Stancin, A. M., J. D. Gleason, R. M. Owen, D. K. Rea, and J. D. Blum (2008b), Piston core record of Late Paleogene (31 Ma) to recent seafloor hydrothermal activity in the Southwest Pacific Basin, *Paleoceanography*, *23*, PA1212, doi:10.1029/2006PA001406.
Swanner, E. D., N. J. Planavsky, S. V. Lalonde, L. J. Robbins, A. Bekker, O. J. Rouxel, M. A. Saito, A. Kappler, S. J. Mojzsis, and K. O. Konhauser (2014), Cobalt and marine redox evolution, *Earth Planet. Sci. Lett.*, *390*, 253–263.
Taylor, S. R., and S. M. McLennan (1985), *The Continental Crust: Its Composition and Evolution*, 312 pp., Blackwell Sci. Publ. Inc., Oxford, U. K.
Taylor, S. R., S. M. McLennan, and M. T. McCulloch (1983), Geochemistry of loess, continental crustal composition and crustal model ages, *Geochim. Cosmochim. Acta*, *47*, 1897–1905.
Thurocszy, C. E., M. Boye, and R. Lonso (2010), Dissolution of cobalt and zinc from natural and anthropogenic dusts in seawater, *Biogeosciences*, *7*, 1927–1936.
van de Flierdt, T., M. Frank, A. N. Halliday, J. R. Hein, B. Hattendorf, D. Günther, and P. W. Kubik (2004), Deep and bottom water export from the Southern Ocean to the Pacific over the past 38 million years, *Paleoceanography*, *19*, PA1020, doi:10.1029/2003PA000923.
Von Damm, K. V., J. M. Edmond, B. Grant, B. Walden, and R. F. Weiss (1985), Chemistry of submarine hydrothermal solutions at 21 N, East Pacific Rise, *Geochim. Cosmochim. Acta*, *49*, 2197–2220.
Zhou, L., and F. T. Kyte (1992), Sedimentation history of the South Pacific pelagic clay province over the last 85 million years inferred from the geochemistry of Deep Sea Drilling Project Hole 596, *Paleoceanography*, *7*, 441–465.
Ziegler, C. L., and R. W. Murray (2007), Geochemical evolution of the central Pacific Ocean over the past 56 Myr, *Paleoceanography*, *22*, PA2203, doi:10.1029/2006PA001321.
Ziegler, C. L., R. W. Murray, S. A. Hovan, and D. K. Rea (2007), Resolving eolian, volcanogenic, and authigenic components in pelagic sediment from the Pacific Ocean, *Earth Planet. Sci. Lett.*, *254*, 416–432.
Ziegler, C. L., R. W. Murray, T. Plank, and S. R. Hemming (2008), Sources of Fe to the equatorial Pacific Ocean from the Holocene to Miocene, *Earth Planet. Sci. Lett.*, *270*, 258–270.